A Physiologically Based Pharmacokinetic Model for 2,4-Toluenediamine Leached from Polyurethane Foam-covered Breast Implants

Hoan-My Do Luu, Joseph C. Hutter, and Harry F. Bushar

Center For Devices and Radiological Health, Food and Drug Administration, Rockville, MD 20852 USA

Physiologically based pharmacokinetic (PBPK) modeling was used to assess the low-dose exposure of patients to the carcinogen 2,4-toluenediamine (2,4-TDA) released from the degradation of the polyester urethane foam (PU) used in Meme silicone breast implants. The tissues are represented as five compartments: liver, kidney, gastrointestinal tract, slowly perfused tissues (e.g., fat), and richly perfused tissues (e.g., muscle). The PBPK model was fitted to the plasma and urine concentrations of 2,4-TDA and its metabolite 4-AAT (4-*N*-acetyl-2-amino toluene) in rats given low doses of 2,4-TDA intravenously and subcutaneously. The rat model was extrapolated to simulate oral and implant routes in rats. After adjusting for human physiological parameters, the model was then used to predict the bioavailability of 2,4-TDA released from a typical 4.87-g polyester urethane foam implant found in a patient who weighed 58 kg with the Meme and had the breast implant for 10 years. A quantitative risk assessment for 2,4-TDA was performed and the polyester urethane foam did present an unreasonable risk to health for the patient. *Key words*: implant, PBPK, physiologically based pharmacokinetic model, polyester urethane, risk assessment, 2,4-toluenediamine. *Environ Health Perspect* 106:393–400 (1998). [Online 10 June 1998] *http://ehpnet1.niehs.nih.gov/docs/1998/106p393-400luu/abstract.html*

Polyurethanes have been used in breast implant covers, pacemaker leads, hemodialyzer potting material, and other medical applications. The degradation of polyurethanes *in vivo* has long been a concern due to both the release of potentially harmful materials as well as mechanical failure. The composition of the polyurethane degradation products depends on the original formulation of the polymer. The polyester urethane (PU) foam cover of the Meme breast implant (or Replicon; Surgitek Corporation, Racine, WI) was made from a polyester resin and a 80:20 mixture of 2,4-toluene diisocynate and 2,6-toluene diisocyanate (2,4-TDI, 2,6-TDI) (*1*). One of the degradation products of TDI is 2,4-toluenediamine (2,4-TDA). Data in experimental animals showed that the PU foam cover degraded within 6–12 months of implantation (*2*). This result was consistent with the clinical observations in patients with Meme breast implants (*3,4*). Our own *in vitro* studies indicated that 2,4-TDA was slowly released over time by hydrolytic degradation when PU foam samples were incubated under mild physiological conditions (*5,6*). The amount and rate of 2,4-TDA production observed *in vitro* varied with the conditions of PU foam exposure (*7–9*). The carcinogenicity of 2,4-TDA was studied extensively in mice, rats, and other species (*10–19*). Exposure of patients to this rodent carcinogen, one of the degradation products of Meme breast implants, is a potential health risk (*20–24*).

Physiologically based pharmacokinetic (PBPK) modeling uses physiological parameters such as organ volumes, blood flows, and excretion flows, and chemical specific parameters such as tissue solubility and biotransformation rates. This type of modeling uses these physiological parameters to complete a material balance on the component of interest in the body. An important feature of this type of model is predicting the absorption, distribution, metabolism, and elimination of the simulated chemical. Animal data using one uptake route can be extrapolated to another route and/or from animal species to humans with minor changes to the PBPK model. The extrapolative value of this approach in human health risk assessment has long been used for many drugs and chemicals (*25–28*).

The objectives of this study were to develop a PBPK model to simulate the fate of low-dose exposure of 2,4-TDA from implant degradation and assess the potential health risk in patients with Meme PU foam-covered silicone breast implants. The PBPK model was initially developed to fit experimental data obtained in rats injected intravenously (iv) and subcutaneously (sc) with low doses of 2,4-TDA, 0.54 mg/kg and 0.44 mg/kg, respectively (*29*). Once the PBPK model adequately simulated the fate of 2,4-TDA and its metabolite by different routes of exposure, the model was scaled up to a human PBPK model using appropriate physiological and pharmacokinetic parameters. The model was solved numerically using an adaptive grid Runge-Kutta method in the Mathcad PLUS 6.0 software package (MathSoft, Cambridge MA). Using sensitivity analysis, we evaluated the rat model and determined the rate-limiting steps that changed with doses, routes, and species. Statistical validation of the fit of the experimental rat results to the PBPK model simulation results was performed as described by Krishman and Anderson (*25*). The kinetic behavior of 2,4-TDA and its metabolite were derived from the implant PBPK model for both rats and humans. The simulated results were compared to the available independent data for validation (*10–13,22,29*). Finally, a quantitative risk assessment was performed to assess the potential cancer risks in patients with Meme silicone breast implants.

Methods

PBPK model. The model consists of five tissue compartments: two excreting compartments [kidney and gastrointestinal (GI) tract], slowly perfused tissues (e.g., fat), richly perfused tissues (e.g., muscle), and metabolizing tissue (liver). The model is very similar to styrene and methylene chloride PBPK models (*27,28*). The hydrolytic PU foam degradation rate constant, K_d, was zero order with an experimentally determined value of 88 ng 2,4-TDA/g foam/day as previously reported (*5,6*). The degradation of the PU foam *in vivo* was assumed to produce only one product, 2,4-TDA (*29*). The PBPK model for 2,4-TDA accounts for hepatic metabolism, which is known to produce an active metabolite (*18,19*). Although there were at least eight known metabolites of 2,4-TDA in the liver, 2,4-TDA was assumed only to have one metabolite, 4-acetylamino-2-aminotoluene (4-AAT), in this model for simplicity (*19,29*). The rate of production of 4-AAT was controlled by an adjustable selectivity in the model (*19*). The selectivity was defined as the fraction of metabolites of 2,4-TDA that were converted to 4-AAT. The value of the selectivity was set according

Address correspondence to H-M.D. Luu, HFZ-150, Office of Science and Technology, Center For Devices and Radiological Health, 12725 Twinbrook Parkway, Rockville, MD 20852 USA.

The authors wish to thank Leroy Schroeder, Ronald Brown, and Meyer Katzper for helpful suggestions in this investigation, and Wen-Jau Chiou for statistical analyses of the data. Without their help, this study would not have been possible.

The opinions or assertions about specific products identified by brand name herein are the private views of the authors and are not to be construed as conveying either an official endorsement or criticism by the U.S. Department of Health and Human Services or the Food and Drug Administration.

Received 17 September 1997; accepted 3 February 1998.

to the published fraction of metabolites that were 4-AAT (0.32) (*19*). The metabolite 4-AAT was also distributed, metabolized to an unknown product, and excreted (*11*). 2,4-TDA was modeled to be an equilibrium system between protein-bound and free 2,4-TDA, with the ratio of bound to free kept constant so that 9.7% of the 2,4-TDA was free, as shown in the initial experimental rat plasma samples (*29*). As shown in Figure 1, blood of uniform composition exiting the mix point flowed through the implant into the arterial circuit. The uniformly mixed arterial blood was then distributed to other compartments in the body. The blood flow rate to each compartment was determined from published physiological measurements (*26*). The distribution coefficient (D), which related to the blood/tissue partition coefficient (P), was defined as the ratio of the concentration of 2,4-TDA or metabolite in the tissue to its emergent venous blood concentration. The 2,4-TDA (and 4-AAT) distribution coefficients and metabolism rate constants were obtained from previously published radioactive distribution studies in rats and mice (*11–13*). Venous blood exits each compartment at equilibrium with the tissue in that compartment. Unlike the arterial circuit, the blood exiting each compartment in the venous circuit did not have a uniform composition of 2,4-TDA or its metabolite. Before the blood was returned to the implant and arterial circuit, it was completely mixed at the mix point.

All of the 2,4-TDA was metabolized in the liver, and the metabolites were then returned to the venous blood for circulation to the other compartments for subsequent absorption, further metabolism, or excretion. Metabolites or 2,4-TDA can be excreted in either the urine or the feces (*19*). The complete model equations are discussed in the Appendix. Table 1 lists the range of the parameters used in the model for both rats and humans (*26*).

Experimental data. Three sets of independent experimental data were used to calibrate the model (*29*).

After iv injection with 0.52 mg/kg 2,4-TDA, blood samples were collected from five female CDF (F-344)/Crl rats at various time intervals (0.05, 0.15, 0.25 hr, etc.) up to 48 hr after dosing. Both the 2,4-TDA and 4-AAT plasma results were measured by a validated GC/MS analytical method with a detection limit of 0.1 ng/ml. These results were used to fit the metabolism parameters for both 2,4-TDA and 4-AAT in the model. As discussed previously, distribution coefficients were assigned from radioactive distribution studies (*11,12,16*).

Urine was obtained for analysis after female CDF (F-344) CRL BR rats (n = 5) received a single sc injection of 2,4-TDA (0.44 mg/kg). The mean fraction of 2,4-TDA excreted unchanged was 0.22% (range 27–51 ng/ml). The corresponding concentration of urinary 4-AAT recovered was less than 1% (range 103–188 ng/ml) within 48 hr after dosing. These results were used to set the urine/feces excretion distribution coefficients.

In another study, a ^{14}C-labeled foam was synthesized from ^{14}C-TDI comparable to the foam used in the manufacture of Meme breast implants; this ^{14}C-labeled foam was implanted sc in young female rats at a dose comparable to 80 mg/kg. Radioactivity was evaluated in urine, feces, and selected tissues at various intervals post implantation (1, 4, 12, and 24 hr, and 7, 15, 21, 28, and 56 days). At 56 days, the cumulative excretion of radioactive material amounted to 2% (urinary 0.9% and

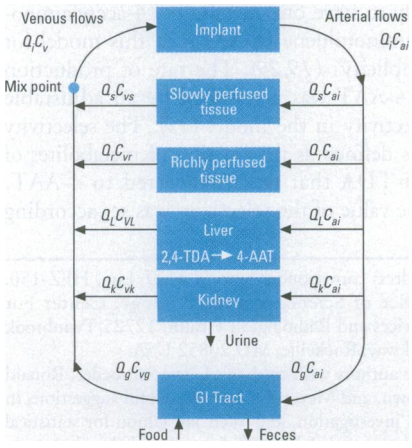

Figure 1. Flow diagram of the physiologically based pharmacokinetic (PBPK) model. Abbreviations: Q_j, jth blood flow rate (ml/hr), C, 2,4-toluenediamine (2,4-TDA) concentration (mol/ml); *a*, arterial blood; *g*, gastrointestinal (GI) tract; *i*, mixed blood, *k*, kidney; *L*, liver; *r*, richly perfused tissues; *s*, slowly perfused tissues; *v*, venous blood; 4-AAT, 4-*N*-acetyl-2-amino toluene.

Table 1. Values of the parameters used in the physiologically based pharmacokinetic (PBPK) model (*26*)

	Rat		Human	
Compartment	Blood flow (ml/hr)	Compartment volume (ml)	Blood flow (ml/hr)	Compartment volume (ml)
Slowly perfused tissue	55.2	19.1	26,520	13,562
Richly perfused tissue	2,640	144.9	123,200	40,672
Liver	912	8.8	71,760	1,419
Kidney	702	1.7	46,800	243
Gastrointestinal tract	696	6.0	43,680	948
Total cardiac output	5,005	–	312,000	–
Range of cardiac output (published, resting)	4,980–8,040	–	$2.8–4 \times 10^5$	–

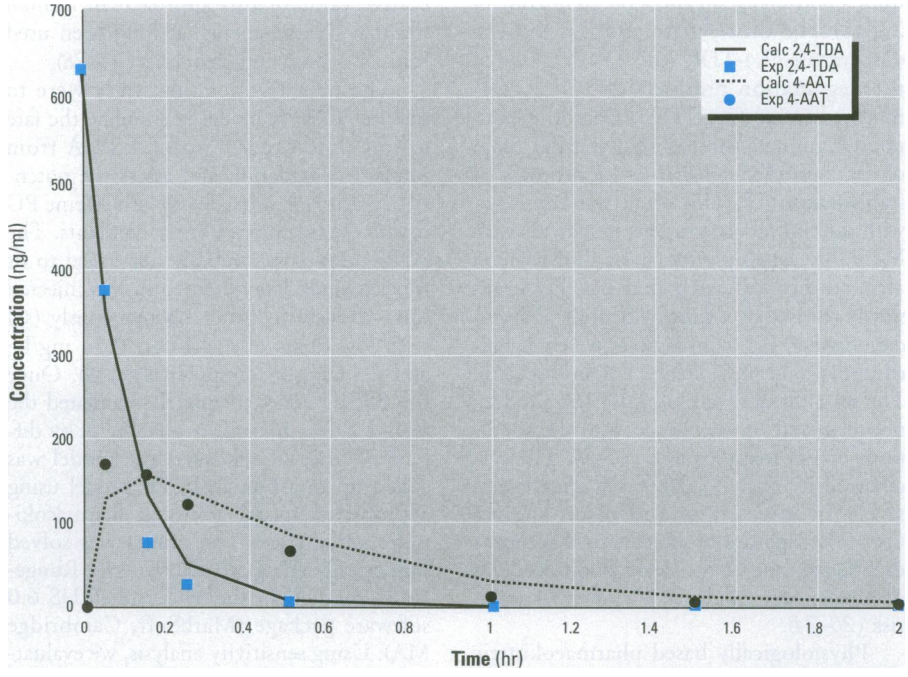

Figure 2. Fitted results of the plasma concentrations for a 0.52 mg/kg iv bolus injection. Abbreviations: 2,4-TDA, 2,4-toluenediamine; 4-AAT, 4-*N*-acetyl-2-amino toluene; Calc, calculated; Exp, experimental.

fecal 1.1%) of the implanted dose. The presence of radioactive material in rat urinary and fecal excreta at 56 days indicated a slow and continued degradation of implanted PU foam *in vivo*. These results were used to verify our fitted excretion data as discussed above and as an independent check of the tissue distribution parameters.

Results

Calibration using iv bolus and sc administration of a low dose of 2,4-TDA in the rat. The fitted experimental plasma concentrations following iv injection of a 0.52-mg/kg dose 2,4-TDA are shown in Figure 2. 2,4-TDA plasma levels decreased rapidly following iv administration in rats. Although this dose would be expected to produce a blood concentration of 6,500 ng/ml in the rat, the maximum initial plasma concentration was 633 ng/ml, indicating that 2,4-TDA was rapidly bound to plasma proteins confirming previous observations (*22*). The blood flow parameters; and compartment volumes were set from published physiological parameters; the tissue distribution coefficients were obtained from published radioactive distribution studies as discussed earlier (*11–13, 26*). Even with these constraints, the model was robust enough to accurately correlate the experimental results using only the metabolism parameters for both 2,4-TDA and 4-AAT.

From the material balance results, the area under the serum concentration time curve (AUC) of 2,4-TDA from time zero to infinity was determined to be 62.176 ng/hr/ml, the total body clearance (Cl) was 8,363 ml/hr, and the volume of distribution (V_d) was 1,379 ml/kg (*30*). The elimination half life ($t_{1/2}$) of free 2,4-TDA in the plasma was 0.074 hr due to its extensive binding to plasma proteins (*22*). The protein bound 2,4-TDA is in equilibrium with the free 2,4-TDA, which is biologically active. The extent that protein binding influences the delivery of free 2,4-TDA to the target organ may change in certain human disease states (*30*). After the first 6 hr, the plasma levels of 2,4-TDA dropped to a very low value below the analytical detection limits. As shown, most of the administered dose of 2,4-TDA was rapidly metabolized, and very little was excreted or absorbed (0.22%). The urinary concentration of 4-AAT reached nearly 500 ng/ml, well above detection limits, even though less than 0.3% (weight) of the original dose was excreted. Thus, the predicted cumulative concentrations of 4-AAT excreted in the urine were well fitted to the urine analysis data obtained from the rat subcutaneous study (*29*).

Kinetics of 2,4-TDA from implant simulation in the rat. The simulated implant results in the rat are shown in Figures 3 and 4. Unlike the intravenous cases, the implant provided a continuous low-level dose of 2,4-TDA to the tissues. The predicted plasma steady state concentration (C_{ss}) of 2,4-TDA was only 3.4×10^{-5} ng/ml. Therefore, we do not recommend the use of free plasma 2,4-TDA to monitor the breakdown of PU foam. The plasma level of 4-AAT was also too low to be detected. Table 2 summarizes the calculated pharmacokinetic parameters of free 2,4-TDA and 4-AAT following three different routes of administration of a low dose in the rat.

Kinetics of 2,4-TDA from implant simulation in the human. The physiological and biochemical parameters that were used to adjust the rat model to a human model are summarized in Tables 1 and 3. The tissue distribution coefficients, which were assumed to be the same for both rats and humans, were obtained from the literature (*11–13*). The metabolism parameter V_{max} was extrapolated by scaling on the basis of (body weight)$^{0.7}$, where 45.27 was the scaling factor between rats and humans [scaling factor = $(58/0.250)^{0.7}$] (*27*). The results of the human PBPK simulation are shown in Table 2. The model predicted that the C_{ss} of free 2,4-TDA and 4-AAT in plasma of a patient with 4.87 g Meme breast implants and body weight of 58 kg would be 1.55×10^{-4} ng/ml and 2.58×10^{-4} ng/ml, respectively (values for the rat would be 3.40×10^{-5} ng/ml and 5.77×10^{-5} ng/ml, respectively). The lower serum concentration values in the rat were a direct result of higher metabolism because

Table 2. Comparison of 2,4-TDA iv bolus, feeding, and implant results in rat and human models

	Rat, 0.52 mg/kg iv bolus	Rat, 0.52 mg/kg feeding	Rat, 0.021 g implant	Human, 4.872 g implant
Percent original dose accumulated				
Feces	0.053	0.052	0.047	0.019
Urine	0.224	0.220	0.239	0.309
Liver	7.5×10^{-5}	0.017	0.514	1.75
Kidney	0.024	0.025	0.531	1.48
RP tissue	1.2×10^{-4}	0.113	2.789	15.4
SP tissue	3.3×10^{-4}	0.043	0.701	9.55
GI tract	4.9×10^{-4}	0.099	1.973	6.06
Plasma clearance calculations				
AUC (ng/hr/ml)	62.179	58.951	1.98×10^{-4}	0.846
2,4-TDA $t_{1/2}$ (hr)	0.074	0.776	Lifetime	Lifetime
Clearance (ml/hr/kg)	8,360	8,820	9,320	2,175
V_d (ml/kg)	1,379	12,570	54,900	11,770
4-AAT $t_{1/2}$ (hr)	0.389	0.863	Lifetime	Lifetime

Abbreviations: iv, intravenous; AUC, area under the curve, free 2,4-toluene diamine concentration in plasma vs. time; V_d, volume of distribution; 2,4-TDA, 2,4-toluenediamine; 4-AAT, 4-*N*-acetyl-2-amino toluene; RP, richly perfused; SP, slowly perfused; GI, gastrointestinal.

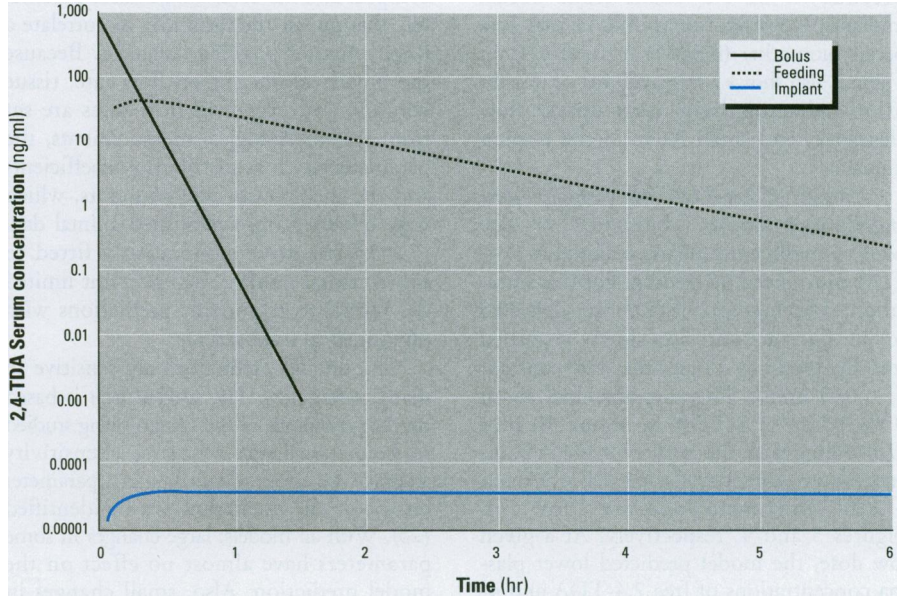

Figure 3. Comparison of the plasma concentrations of 2,4-TDA following the intravenous bolus injection, feeding, and implant in the rat. Abbreviations: 2,4-TDA, 2,4-toluenediamine; 4-AAT, 4-*N*-acetyl-2-amino toluene.

Table 3. Metabolism and excretion parameters used in the physiologically based pharmacokinetic (PBPK) model

Metabolism and excretion parameters	Rat value	Human value
V_{max} (mol/hr)[a]	0.12	0.54
k_m (mol/ml)	7×10^{-7}	7×10^{-7}
V_{mmax} (mol/hr)[a]	0.01	0.46
k_{mm} (mol/ml)	3×10^{-7}	3×10^{-7}
Urine flow (ml/hr)	0.75	90
2,4-TDA D_{urine}	0.5	0.5
4-AAT D_{urine}	10.0	10.0
Feces flow (ml/hr)	0.60	18
Blood volume (ml)	20.0	4,700
2,4-TDA distribution coefficient		
Slowly perfused tissue	1.0	1.0
Richly perfused tissue	1.0	1.0
Liver	5.0	5.0
Kidney	3.0	3.0
GI tract	5.0	5.0
4-AAT distribution coefficient		
Slowly perfused tissue	1.0	1.0
Richly perfused tissue	0.4	0.4
Liver	1.0	1.0
Kidney	10.0	10.0
GI tract	10.0	10.0

Abbreviations: V_{max}, 2,4-TDA metabolism parameter (mol/hr); V_{mmax}, 4-AAT metabolism parameter (mol/hr); k_m, 2,4-TDA metabolism parameter (mol/ml); k_{mm}, 4-AAT metabolism parameter (mol/ml); D_{urine}, distribution coefficient for 2,4-TDA or 4-AAT in urine (urine concentration/tissue concentration.

[a]Scale-up factor human/rat based on body mass (58 kg/0.25 kg)$^{0.7}$ (*27*).

the distribution coefficients and relative excretions were the same in these calculations. In the human, this corresponds to a plasma level of 16×10^{-4} ng/ml of total 2,4-TDA (free + conjugated; 9.7% free). Similar to the rat implant we do not recommend using free plasma 2,4-TDA to monitor the breakdown of PU foam from breast implants. However, urinary 4-AAT may be a better biomarker (0.309% or 0.96 ng/ml). Table 2 also shows a large volume of distribution indicating high tissue uptake, low clearance, and small AUC in the human implant.

Kinetics of 2,4-TDA following low-dose ingestion in the rat. The model was also used to predict the pharmacokinetics 2,4-TDA introduced by feeding. For this simulation, 0.52 mg/kg 2,4-TDA was delivered to the GI tract and was slowly absorbed into the blood by a first order rate constant of 0.015 min^{-1}. This rate absorbed about 99% of the 2,4-TDA in about 90 min (*16*). Along with the results for the iv bolus and the implant, the plasma 2,4-TDA and 4-AAT concentrations are shown in Figures 3 and 4, respectively. At a given low dose, the model predicted lower plasma concentrations of free 2,4-TDA and 4-AAT following the oral route compared to iv bolus due to slower absorption rate. However, these concentrations persisted for a much longer period of time, so the area under the plasma concentration time curve was equivalent (AUC = 58.95 ng/hr/ml) compared to exposure from the iv route. The 4-AAT urinary concentration reached a maximum of 240 ng/ml after about 1 hr, a very comparable level to the sc result because the 2,4-TDA was introduced gradually in both cases. The cumulative urinary level of 4-AAT was determined to be less than 0.3% (weight) of the original dose following an oral bolus dose of 2,4-TDA.

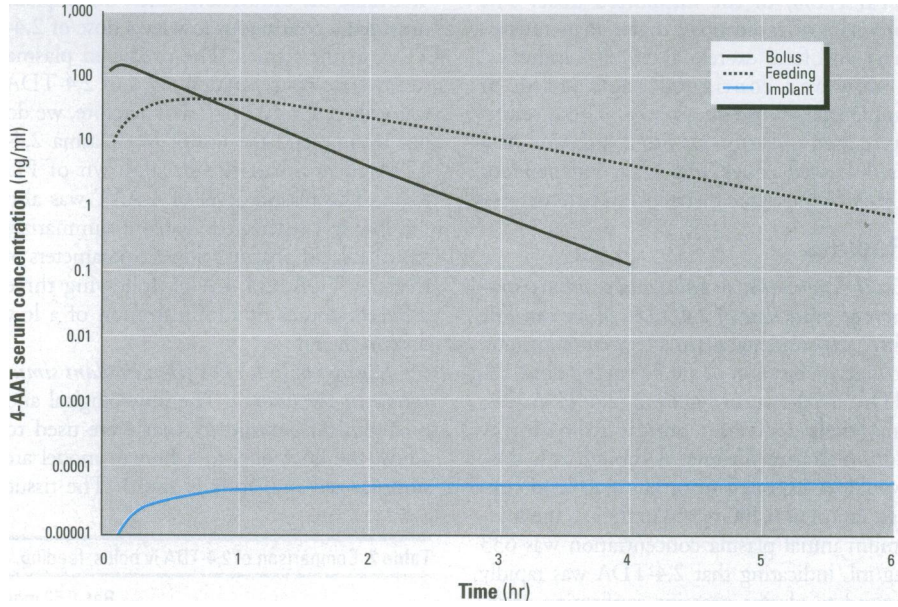

Figure 4. Comparison of the plasma concentrations of 4-*N*-acetyl-2-amino toluene (4-AAT) following the intravenous bolus injection, feeding, and implant in the rat.

Sensitivity analysis. The PBPK model for 2,4-TDA, as shown in the Appendix, is complex and has several adjustable parameters that give it the flexibility to correlate a large range of possible scenarios. Because the blood volume, blood flow rate, tissue volume, and excretion flow rates are set from the physiological measurements, the parameters such as distribution coefficients and the metabolism rate constants, which were obtained from published animal data (*11–13,16*), were subsequently fitted to experimental results. Such restraint limited the model to reasonable predictions with physiological implications.

The model predictions are sensitive to many parameters. The model itself is based on the physiology of the system being studied to keep it realistic. By using a sensitivity analysis, the effect of a change in a parameter on the model prediction can be identified (*25*). With all models, large changes in some parameters have almost no effect on the model prediction. Also, small changes in some parameters have drastic changes in model predictions. Thus, a sensitivity analysis can be used to identify parameters that are critical to be measured by experimental studies. The parameters that are not critical to the model prediction do not require the same degree of experimental effort to quantify for experimental validation of the model. The usefulness of the PBPK approach is to use a mathematical model to predict the results that are difficult or impossible to obtain experimentally (*25*). Thus, the point of the PBPK model is not to predict results at all points in the human or animal body and compare the results to experimental data at all the points, but rather a few key results are predicted, e.g., plasma concentrations and excretion rates, and these are used for a simple validation (*25*). The physiology is used to predict the other unmeasurable points based on the best available data (blood flows, organ volumes, etc.). This simple validation will give substantially more predictive power than simple one- or two-compartment pharmacokinetic models, which are often validated with the same type of very limited data.

Sensitivity analysis identified a few critical model parameters. Both of the metabolism parameters, V_{max} and K_m, which reflect the activity of specific liver enzymes to biotransform 2,4-TDA, were found to be the controlling parameters effecting the excretion and accumulation of 2,4-TDA and its metabolites in each compartment. This is consistent with the mode of action of 2,4-TDA based on the literature (*10–19*). A 100% increase in V_{max} (or decrease in K_m), will result in a 10% decrease in the accumulation of 2,4-TDA in each compartment, a minimal change in its excretion, but nearly a 50% decrease in free plasma concentration. A 50% decrease

in V_{max} (or increase in K_m), will also only result in a 10% increase in accumulation in each compartment, a minimal change in excretion, and a large time lag in the plasma concentration reduction.

In general, as D (distribution coefficient) increases, the accumulation of 2,4-TDA and its metabolites will increase in that compartment while accumulations in other compartments and excretions will decrease to compensate. As expected, because the richly perfused tissue (r) has the largest organ volume as well as the highest percentage of the cardiac output, the value of the distribution coefficient (D_r) also has a significant effect on the model predictions. For example, a 100% increase in D_r will result in nearly 16% reductions in the amount of 2,4-TDA or its metabolites accumulated in the other compartments and a minimal effect on excretion. Similarly, a 50% decrease in D_r will also result in nearly 8% increases in accumulation and a minimal effect on excretion. Similar changes in D_l (liver), D_s (slowly perfused tissue), D_k (kidney), and D_{GI} (GI tract) will result in very minor changes in other compartments. These other distribution coefficients have only minor (1–2%) effects on the tissue distributions overall; thus, even large errors in their estimated values will not change the overall predictions of the model. This relative importance of D_r sensitivity is due to a combination of both organ volume and blood flow. The larger the combination of blood flow and organ volume to a tissue compartment, the more impact changes in the equilibrium distribution coefficient will have on the model output. The uniqueness of the slowly perfused tissue response (e.g., fat tissue) compared to other compartments is the time lag. This compartment has the highest ratio of tissue volume to blood flow rate; thus, changes in the distribution coefficient in this compartment manifest their effects on a slower time scale (2–3 hr), compared to changes in other compartments that manifest themselves in about 10 min.

The kidney and GI tract are unique since they are the only compartments in which excretion occurs. Although changes in the distribution coefficients will have only minor effects on excretion, the values of D_{urine} and D_{feces}, along with the flow rates of urine and feces, have a very significant effect on excretion. However, solubility limitations and physiology of the rat put limits on how high or how low one can make the flow rate of urine and feces.

Statistical analysis. For statistical validation (*25*) of just how well the experimental rat results fitted the PBPK simulation results, the log (base 10) transformed 2,4-TDA rat blood data were shown to follow the same linear model as the log (base 10) transformed 2,4-TDA PBPK model predictions, over the first half hour, i.e., no statistically significant difference for either slope or intercept between the transformed data and the transformed predictions, even at the 10% significance level. For the 4-AAT, the residuals or differences between the log (base 10) transformed 4-AAT rat blood data and the log (base 10) transformed 4-AAT PBPK model predictions from 0.05 to 0.5 hr were shown to have a zero mean, no statistically significant difference from zero even at the 40% significance level, and a 90% tolerance interval with 90% coverage for individual residuals of 43% and 202% for the rat data as percent of model prediction.

Discussion

In the safety evaluation of the PU foam-covered breast implants, it is difficult to assess the carcinogenic potential of the Meme breast implants relative to 2,4-TDA, a mutagen and carcinogen known to be released from the device (*20–24*). The data available for this purpose are generally high-dose feeding (4.7–10.6 mg/kg) animal data (*14–16,18,19*). Therefore, we need pharmacokinetic models that rely on realistic physiological parameters and chemical-specific parameters to be able to extrapolate between high and low doses, different routes of administration, and from animal to human (*25*). The objective of this paper is to use the PBPK model for 2,4-TDA in rats to predict the long-term distribution, excretion, and metabolism of the low-dose infusion cases that are characteristic in humans with breast implant degradation. The PBPK model for 2,4-TDA adequately simulated the experimental 2,4-TDA and 4-AAT rat plasma data (Fig. 2). The fit of the experimental rat results to the PBPK model simulation results was validated statistically as shown earlier (*25*). Table 2 shows the pharmacokinetic data of 2,4-TDA between three simulated routes of exposure in rats. The data obtained from the mass balance studies shed light on how the implant route produces a large volume of distribution (V_d = Dose/C_{max} = 54,900 ml/kg). Such a large V_d reflects high tissue uptake and accumulation of the initial dose of free 2,4-TDA and metabolites in target tissues such as the liver, kidney, and fat (Table 2). As shown, the simulated data obtained in this study agree well with the distribution studies using radiolabeled 2,4-TDA in animals, which indicated the highest accumulation of 2,4-TDA and metabolite in the richly perfused tissue, slowly perfused tissue, GI tract, kidney, and liver (*11–13,16*).

The model also predicts a slow excretion of 2,4-TDA from an implant (5% excreted in urine in the first week and 0.94% excretion in the feces) compared to an iv bolus and oral administration at a given dose, confirming the experimental results obtained following implantation with ^{14}C 2,4-TDA-labeled-foam (80 mg/kg) in which approximately 2% of the total radioactivity was excreted after 56 days (*29*). As shown in Table 2, the PBPK model predicts that the continuous low-dose infusion of 2,4-TDA produced by PU foam hydrolysis from breast implants produces a very small AUC (2×10^{-4} ng/hr/ml). The very small AUC is due to both a slow rate of degradation of the implant, which is assumed in this model to be similar to the rate obtained *in vitro* (88 ng 2,4-TDA/g of foam per day under mild simulated physiological conditions) (*5,6*). In addition, most 2,4-TDA produced from the breakdown of the PU foam cover is extensively bound to plasma protein (9.7% free). The plasma protein binding of 2,4-TDA was obtained experimentally in the rat iv study (90.3% bound).

The model-predicted results in this study confirmed that carcinogenic degradation products that are produced from implanted PU foam are stored in target organs and small amounts are excreted in animals and humans (*2,20–24,29*). Although there is no data available at this time to show a cause and effect relationship between the use of this PU foam and production of cancer in humans, the lifetime duration of exposure of the device, the high tissue uptake, and slow clearance of 2,4-TDA from breast implants are important factors contributing to the potential hazard of 2,4-TDA released from the PU foam-covered breast implants in humans (*30*). Indeed, in distribution studies, the levels in every organ tested at 24 hr was reported to be higher in the rat than in the mouse, indicating more toxicity with slower clearance and larger distribution in rats; this is consistent with the higher cancer rate in rats than in mice (*11–13*).

At a given low dose, the iv bolus and the oral administration have about the same clearance and equivalent AUC as shown in Table 2. In the oral administration, however, a sustained level of 2,4-TDA or metabolite was found in the plasma and tissues, indicating longer residence time (longer $t_{1/2}$) and larger tissue distribution (V_d=12,570 ml/kg) than the iv bolus administration (*16*). 2,4-TDA persists longer in the body following oral administration of a small dose (0.5 mg/kg), confirming the results obtained by Timchalk et al. (*16*). Therefore, the model-predicted data confirm earlier findings that suggest the susceptibility to carcinogenic effects of 2,4-TDA is also dependent on the route of administration that affects 2,4-TDA kinetic behavior and thus the dose to target organs (*16*).

As shown in Figure 4, the predicted steady state plasma concentration (C_{ss}) of free 2,4-TDA in the rat is very low (only 3.4×10^{-5} ng/ml), too low to be detected by the current state of the art analytical instrumentation (detection limits <0.1 ng/ml). However, the pharmacokinetic data derived from this PBPK model can be used to determine the total daily dose and to estimate exposure. The standard pharmacokinetic equation that relates infusion rate, steady state plasma concentration, and clearance of a chemical is as follows:

$$\text{Infusion rate } R = C_{ss} \times \text{Clearance}.$$

This equation predicts the rate of release of free 2,4-TDA from the implants *in vivo* by assuming that the release rate is equivalent to a constant slow infusion. Therefore, in the rat model,

$$\begin{aligned}\text{Release Rate} &= C_{ss} \times \text{Clearance}\\ &= 3.4 \times 10^{-5} \text{ ng/ml} \times 9{,}320 \text{ ml/hr/kg}\\ &= 0.317 \text{ ng/hr/kg}\\ &= 0.317 \times 24 \text{ hr/day}/1{,}000{,}000 \text{ ng/mg}\\ &= 7.60 \times 10^{-6} \text{ mg/kg/day}.\end{aligned}$$

As such, the PBPK model provides a quantitative estimate of exposure that relates both plasma steady state level and clearance rate.

Estimated human health risks from breast implants. Essentially, to estimate human risks, we have to derive the human exposure from the release rate of 2,4-TDA from the breast implants using the results of the human PBPK simulation shown in Table 2. As with the rat, the clearance is calculated using the model by dividing the AUC by the total administered dose (*30*). The model predicts that the C_{ss} of plasma free 2,4-TDA is 1.55×10^{-4} ng/ml (9.7% free) in a patient with 4.87 g PU foam in the Meme breast implants and a body weight of 58 kg. This corresponds to a plasma level of 16×10^{-4} ng/ml of total 2,4-TDA (free + conjugated). Thus, the release rate of 2,4 TDA from the foam is as follows:

$$\begin{aligned}\text{Release Rate} &= 16 \times 10^{-4} \text{ ng/ml} \times 2{,}175 \text{ ml/hr/kg}\\ &= 3.48 \text{ ng/kg/hr}\\ &= 3.48 \times 24 \text{ hr/day}/1{,}000{,}000 \text{ ng/mg}\\ &= 83.52 \times 10^{-6} \text{ mg/kg/day}.\end{aligned}$$

This corresponds to a lifetime average daily dose (LADD) of 11.93×10^{-6} mg/kg/day, assuming that the lifetime of the implant was 10 years (10/70). Therefore,

$$\begin{aligned}\text{Upper Confidence Limit on Risk} &= \text{Potency Factor} \times \text{LADD}\\ &= 0.21 \text{ (mg/kg/day)}^{-1} \times 11.93 \times 10^{-6}\\ &= 2.50 \times 10^{-6}\\ &= 1 \text{ in } 400{,}000.\end{aligned}$$

A potency factor (or slope factor) of 0.21 $(\text{mg/kg/day})^{-1}$ was used for 2,4-TDA (*23*), which results in an estimated excess cancer risk of 1 case in 400,000.

After 2,4-TDA was found as a degradation product of the meme breast implants (*2–9*), a risk assessment was completed (*23,24*). A small increase in lifetime risk of breast cancer (5 in 10 million) was reported, based on a limited *in vitro* rate of release of 2,4 TDA (*23,24*). Recently, based on the measured levels of TDAs in the blood of patients with the Meme PU-covered breast implants, Sepai et al. (*22*) estimated an increased risk of lifetime breast cancer of 149 cases in 1 million, which is approximately 60 times more than the value we obtained in this report using a PBPK model. We believe that the discrepancy comes from Sepai et al. (*22*) calculating the risk using the postimplant plasma levels of total 2,4-TDA (4.4 ng/ml) obtained in patients with the Meme breast implants; these levels were 1,000 times higher than the C_{ss} plasma level of 2,4-TDA obtained in this model. Simply by increasing the rate of the *in vitro* degradation that we used in our simulations by a factor of 1,000, we were able to reproduce the C_{ss} reported by Sepai et al. (*22*). No other changes in parameters are needed. As indicated earlier, to model the release of 2,4-TDA in the rat and human, we used the low rate of degradation of the PU foam obtained *in vitro* using phosphate buffered saline, pH 7.4, at 37°C (88 ng/g/day) in our calculation. The higher plasma levels of total TDA that Sepai et al. (*22*) obtained in patients indicate that the PU foam degrades faster *in vivo* (*2–4*). Although the susceptibilities of the PU foam to water, buffer, oxygen, and enzymes at physiological conditions are known (*2–9*), the actual leach rate of 2,4-TDA *in vivo* is not well documented. Another factor that would affect the bioavailability of 2,4-TDA is plasma protein binding, which was lower in the clinical study reported by Sepai et al. (*22*). Thus, PBPK models are limited by available biochemical data such as leaching rate and protein binding, etc; however, they are effective tools for evaluating the safety of 2,4-TDA released from implants.

In general, the risk assessment process has often relied on a number of assumptions that make it imprecise in determining the level of exposure of toxic chemicals (at acceptable risks) to the human population. In this aspect, the PBPK model, which used both physiological parameters (such as organ volumes, blood flows, etc.) and chemical-specific parameters (such as tissue distribution coefficients and biotransformation rates), can be used to predict the kinetics of chemicals and extrapolate between different routes of compound administration and species.

Conclusions

Despite the extreme complexity of the rat, a relatively simple five-compartment PBPK model gives some useful information about the mechanism of toxicity and the route-dependent metabolism of 2,4-TDA.

- The model provides an objective mechanism for determining the bioavailable dose of the parent compound and/or its active carcinogenic metabolite(s) at target organs, which are inaccessible experimentally.
- The plasma level of free 2,4-TDA should not be used as a biological marker for polyurethane foam degradation because of its extensive protein binding.
- The low release rate of 2,4-TDA from implant foam degradation will produce the characteristic distribution and excretion similar to a low dose (0.5 mg/kg) iv bolus or feeding, but with a longer half-life and a larger volume of distribution, which indicates higher accumulation in the body.
- Although the model has several adjustable parameters, the only really important parameters are the metabolism rate constants V_{max} and K_m and the distribution coefficient in the richly perfused tissues. Other parameters such as the equilibrium distribution coefficients in other compartments did not affect the 2,4-TDA disposition significantly. Physiological limits put restraints on many other parameters to keep the model predictions realistic.
- By determining V_{max} and K_m as rate limiting steps in the biotransformation of 2,4-TDA, the PBPK model facilitates the extrapolation across species and from one route to another.

The PBPK results for humans can be used to predict an excess lifetime risk of breast and liver cancer of 1 in 400,000 in patients with the PU foam-covered breast implants. At our present stage, the risk associated with exposure to a chemical cannot be accurately characterized by a single number or even a range of numbers. The use of this type of PBPK method will provide the Food and Drug Administration (FDA) with tools for the interpretation of data within a single species, for comparison of pharmacokinetic result and effects between different species, and to improve the prediction of human effects of many chemicals that are leached or degraded at a low dose rate from medical implants. The model is most useful in this case when the plasma level of the parent compound (e.g., 2,4-TDA) and/or its main metabolite are below the limit of detection of current analytical methods (0.1 ng/ml) due to plasma protein binding. Further research is needed on the biochemical and physicochemical characteristics of importance to biokinetic modeling.

References and Notes

1. Scott Paper Co. Polymer Foam Modification. US patent 858,127. 7 June 1957.
2. Picha GJ, Goldstein JA, Stohr E. Natural-Y Meme polyurethane versus smooth silicone: analysis of the soft-tissue interaction from 3 days to 1 year in the rat animal model. Plast Reconstr Surg 85(6):903–916 (1990).
3. Smahel J. Tissue reactions to breast implants coated with polyurethane. Plast Reconstr Surg 61(1):80–85 (1978).
4. Melmed EP. Polyurethane implants: a 6-year review of 416 patients. Plast Reconstr Surg 82(2): 285–290 (1988).
5. Luu HMD, White KD. In-vitro detection of 2,4- and 2,6-TDA as degradation products of a polyesterurethane foam. Poly Degrad Stabil 42:245–251 (1993).
6. Luu HMD, Biles J, White KD. Characterization of polyesterurethane degradation Products. J Appl Bio Mater 5:1–7 (1994).
7. Amin P, Willie J, Slah K, Kydonieus A. Analysis of the extractive and hydrolytic behavior of microthane poly(ester-urethane) foam by high pressure liquid chromatography. J Biomed Mater Res 27:655–666 (1993).
8. Batich C, Williams J, King R. Toxic hydrolysis product from a biodegradable foam implant. J Biomed Mater Res 23:311–319 (1989).
9. Benoit MF. Degradation of polyurethane foams used in the Meme breast implant. J Biomed Mater Res 27:1341–1348 (1993).
10. Glinsukon T, Benjamin T, Grantham PH, Weisburger EK, Roller PP. Enzymic N-Acetylation of 2,4-toluenediamine by liver cytosols from various species. Xenobiotica 5(8):475–483 (1975).
11. Grantham PH, Mohan L, Benjamin T, Roller PP, Miller JR, Weisburger EK. Comparison of the metabolism of 2,4-toluenediamine in rats and mice. J Envron Pathol Toxicol 3:149–166 (1979).

Appendix

The model is a system of coupled ordinary differential equations which solve the material balances for both 2,4-TDA and 4-AAT. These equations are derived from the flow chart shown in Figure 1.

The equations for each compartment follow for 2,4-TDA:

Implant

$$C_{ai} = \frac{Q_i C_v (1+K) + k_0 m_i + \Lambda}{Q_i (1+K)} \quad (1)$$

For the IV bolus injection if $t \le t_{inj}$

$$\Lambda = Q_{inj}\, C_{inj} \quad (2)$$

For the IV bolus if $t > t_{inj}$

$$\Lambda = 0 \quad (3)$$

Slowly perfused tissue

$$\frac{dC_s}{dt} = \frac{Q_s}{V_s} C_{ai}(1+K) - \frac{Q_s C_s}{V_s D_s}(1+K) \quad (4)$$

Richly perfused tissue

$$\frac{dC_r}{dt} = \frac{Q_r}{V_r} C_{ai}(1+K) - \frac{Q_r C_r}{V_r D_r}(1+K) \quad (5)$$

Liver

$$\frac{dC_L}{dt} = \frac{Q_L}{V_L} C_{ai}(1+K) - \frac{Q_L C_L}{V_L D_L}(1+K) - \frac{\frac{V_{max}}{V_L}\frac{C_L}{D_L}}{k_m + \frac{C_L}{D_L}} \quad (6)$$

Kidney

$$\frac{dC_k}{dt} = \frac{Q_k}{V_k} C_{ai}(1+K) - \frac{Q_k C_k}{V_k D_k}(1+K) - \frac{Q_{urine} D_{urine} C_k}{V_k} \quad (7)$$

GI tract

$$\frac{dC_g}{dt} = \frac{Q_g}{V_g} C_{ai}(1+K) - \frac{Q_g C_g}{V_g D_g}(1+K) + \frac{k_a}{V_g} D_o \exp(-k_a t) - \frac{Q_{feces} D_{feces} C_g}{V_g} \quad (8)$$

For the metabolite 4-AAT, the following equations apply:

Slowly perfused tissue

$$\frac{dM_s}{dt} = \frac{Q_s}{V_s} M_{ai} - \frac{Q_s M_s}{V_s D_{ms}} \quad (9)$$

Richly perfused tissue

$$\frac{dM_r}{dt} = \frac{Q_r}{V_r} M_{ai} - \frac{Q_r M_r}{V_r D_{mr}} \quad (10)$$

Liver

$$\frac{dM_L}{dt} = \frac{Q_L}{V_L} M_{ai} - \frac{Q_L M_L}{V_L D_{mL}} + \frac{Sel\,\frac{V_{max}}{V_L}\frac{C_L}{D_L}}{k_m + \frac{C_L}{D_L}} - \frac{\frac{V_{mmax}}{V_L}\frac{M_L}{D_{mL}}}{k_{mm} + \frac{M_L}{D_{mL}}} \quad (11)$$

Kidney

$$\frac{dM_k}{dt} = \frac{Q_k}{V_k} M_{ai} - \frac{Q_k M_k}{V_k D_{mk}} - \frac{Q_{urine} D_{murine} M_k}{V_k} \quad (12)$$

GI tract

$$\frac{dM_g}{dt} = \frac{Q_g}{V_g} M_{ai} - \frac{Q_g M_g}{V_g D_{mg}} - \frac{Q_{feces} D_{feces} M_g}{V_g} \quad (13)$$

For 2,4-TDA at the mix point

$$C_v = \frac{\frac{Q_s C_s}{D_s} + \frac{Q_r C_r}{D_r} + \frac{Q_L C_L}{D_L} + \frac{Q_k C_k}{D_k} + \frac{Q_g C_g}{D_g}}{Q_i} \quad (14)$$

For 4-AAT at the mix point

$$M_{ai} = \frac{\frac{Q_s M_s}{D_{ms}} + \frac{Q_r M_r}{D_{mr}} + \frac{Q_L M_L}{D_{mL}} + \frac{Q_k M_k}{D_{mk}} + \frac{Q_g M_g}{D_{mg}}}{Q_i} \quad (15)$$

Nomenclature

a = arterial blood
g = gastrointestinal tract
i = mixed
k = kidney
L = liver
m = 4-AAT metabolite
r = richly perfused tissue
s = slowly perfused tissue
v = venous blood

(continued next page)

Dependent variables

C_j = jth 2,4-TDA concentration (mol/ml; j = a, g, i, k, L, m, r, s, or v)

M_j = jth 4-AAT concentration (mol/ml)

Independent variable

t = time (hr)

Parameters

C_{inj} = concentration of 2,4-TDA in IV bolus injection (mol/ml)

D_j = jth distribution coefficient (tissue concentration/venous blood concentration)

D_{urine} = distribution coefficient for 2,4-TDA in urine (urine concentration/tissue concentration)

D_{murine} = distribution coefficient for 4-AAT in urine (urine concentration/tissue concentration)

D_{feces} = distribution coefficient in feces (feces concentration/tissue concentration)

D_o = dose of 2,4-TDA in feeding (mol)

K = ratio of bound 2,4-TDA to free 2,4-TDA in blood

k_a = GI absorption rate constant for 2,4-TDA (hr^{-1})

k_m = 2,4-TDA metabolism parameter (mol/ml)

k_{mm} = 4-AAT metabolism parameter (mol/ml)

k_0 = zero order implant degradation constant for 2,4-TDA production (mol/hr/g implant)

m_i = mass of implant (g)

Q_j = jth blood flow rate (ml/hr)

Q_{urine} = urine flow rate (ml/hr)

Q_{feces} = feces flow rate (ml/hr)

Q_{inj} = flow rate of IV bolus injection (ml/hr)

Sel = selectivity for production of 4-AAT from total 2,4-TDA metabolites (0.32) *(24)*

t_{inj} = duration of IV bolus injection (hr)

V_j = jth compartment volume (ml)

V_{max} = 2,4-TDA metabolism parameter (mol/hr)

V_{mmax} = 4-AAT metabolism parameter (mol/hr)

12. Waring RH, Pheasant AE. Some phenolic metabolites of 2,4-toluenediamine in the rabbit, rat, and guinea pig. Xenobiotica 6(4):257–262 (1976).
13. Weisburger EK, Russfield AB, Homburger F, Weisburger JH, Boger E, Van Dongen CG, Chu KC. Testing of twenty-one environmental aromatic amines or derivatives for long term toxicity or carcinogenicity. J Environ Path Toxicol 2:325–356 (1978).
14. Ito N, Hiasa Y, Konishi Y, Marugami M. The development of carcinoma in liver of rats treated with M-toluylenediamine and the synergistic and antagonistic effects with other chemicals. Cancer Res 29(5): 1137–1145 (1969).
15. National Cancer Institute. Bioassay of 2,4-Diaminotoluene for Possible Carcinogenicity. NCI Technical Report Series No.162. Bethesda, MD:National Cancer Institute, 1979.
16. Timchalk C, Smith FA, Bartels MJ. Route-dependent comparative metabolism of [^{14}C]toluene 2,4-diisocyanate and [^{14}C]toluene 2,4-diamine in Fisher 344 rats. Toxicol Appl Pharmacol 124:181–190 (1994).
17. Kadlubar FF, Hammons GJ. The role of cytochrome P-450 in the metabolism of chemical carcinogens. In: Mammalian Cytochromes P-450, vol II (Guengerich FP, ed). Boca Raton, FL:CRC Press, 1987;81–130.
18. IARC. 2,4-Diaminotoluene. In: IARC Monographs on the Evaluation of Carcinogenic Risk of Chemicals to Man. Vol 16: Some Aromatic Amines and Related Compounds—Hair Dyes, Colouring Agents and Miscellaneous Industrial Chemicals. Lyon:International Agency for Research on Cancer, 1978;83–95.
19. WHO. Diaminotoluenes. Environmental Health Criteria No 74. Geneva:World Health Organization, 1987.
20. Chan SC, Birdsell DC, Gradee CY. Detection of toluenediamines in the urine of a patient with polyurethane covered breast implants. Clin Chem 37(5):756–758 (1991).
21. Chan SC, Birdsell DC, Gradee CY. Urinary excretion of free toluenediamines in a patient with polyurethane-covered breast implants. Clin Chem 37(12):2143–2145 (1991).
22. Sepai O, Henschler D, Czech S, Eckert P, Sabbioni G. Exposure to toluenediamines from polyurethane-covered breast implants. Toxicol Lett 77:371–378 (1995).
23. Food and Drug Administration. CDRH Toxicology Risk Assessment Committee Report on Polyester Polyurethane Foam Covering of Silicone Gel Filled Breast Implants. FDA Memorandum, 22 July 1991.
24. Expert Panel of the Canadian Medical Association. Safety of polyurethane-covered breast implants. Can Med Assoc J 145:1125–1128 (1991).
25. Krishnan K, Anderson ME. Physiologically based pharmacokinetic modeling in toxicology. In: Principles and Methods of Toxicology (Hayes WA, ed). 3rd ed. New York: Raven Press, 1994;149–188.
26. Brown RP, Delp MD, Lindstedt SL, Rhomberg LR, Beliles RP. Physiological parameter values for physiologically based pharmacokinetic models. Toxicol Ind Health 13:407–484 (1997).
27. Ramsey JR, Anderson ME. A physiologically based description of the inhalation pharmacokinetics of styrene in rats and humans. Toxicol Appl Pharmacol 73:159–175 (1984).
28. Anderson ME, Clewell HJ, Gargas ML, Smith FA, Reitz RH. Physiologically based pharmacokinetics and the risk assessment process for methylene chloride. Toxicol Appl Pharmacol 87:185–205 (1987).
29. FDA. Discretionary Postmarket Surveillance Protocol for the Meme and Replicon Polyester/ Polyurethane-covered Mammary Products. DPS 920001. Rockville, MD:Food and Drug Administration, 1992.
30. Chasseaud LF. Role of toxicokinetics in toxicity testing. In: Drug Toxicokinetics (Welling P, Iglesia FA, eds, Drug and Chemical Toxicology, Vol 9. New York:Marcel Dekker, Inc. 1993;105–142.